Chemical Physics Impact (2023) 100306

Contents lists available at ScienceDirect

Chemical Physics Impact

journal homepage: www.elsevier.com

Sensing the formaldehyde pollutant by an enhanced BNC_{18} Fullerene: DFT outlook

M. Da'i [a, *], M. Mirzaei [b], F. Toiserkani [c], S.M. Mohealdeen [d], Y. Yasin [e], M.M.S. Bekhit [f], R. Akhavan-Sigari [g, 8]

[a] Faculty of Pharmacy, Universitas Muhammadiyah Surakarta, Surakarta, Indonesia
[b] Independent Researcher
[c] School of Polymer Science and Polymer Engineering, The University of Akron, Akron, OH 44325, United States
[d] Department of Radiology & Sonar Techniques, Al-Noor University College, Nineveh, Iraq
[e] Medical Technical College, Al-Farahidi University, Iraq
[f] Department of Pharmaceutics, College of Pharmacy, King Saud University, Riyadh 11451, Saudi Arabia
[g] Department of Neurosurgery, University Medical Center Tuebingen, Germany
[8] Department of Health Care Management and Clinical Research, Collegium Humanum Warsaw Management University Warsaw, Poland

ARTICLE INFO

Keywords:
Chemical pollutant
Detection
Fullerene
Interaction
Surface decoration

ABSTRACT

An enhanced boron nitrogen decorated carbon fullerene with the formula BNC_{18} (BNC) was investigated for sensing the formaldehyde (FMA) pollutant. Density functional theory (DFT) calculations were performed to optimize the pure C fullerene and the BNC one to prepare a comparative study of facile detection of FMA substance through the formation of FMA@C and FMA@BNC complexes. The details of complexes were re-recognized by the additional quantum theory of atoms in molecule (QTAIM) analyses, in which the formations of both of FMA@C and FMA@BNC were confirmed. However, the BN-decoration enhancement provided a better interacting surface for the BNC fullerene towards the FMA substance in comparison with the pure C fullerene. Moreover, the electronic molecular orbitals features indicated a significant sensing function for the BNC model by improving the semiconductivity for recognizing the adsorbed substance. In this regard, the BNC fullerene was found suitable for successfully approaching two terms of "recovery time" and "conductance rate" for sensing the FMA pollutant.

Introduction

It has been found that the innovation of nano materials and technologies encouraged the researches to work on this novel concept for developing new functions and applications for various fields of scientific and industrial areas [1–4]. Based on the extensive performed works, the nanostructures have been seen very useful to show significant structural and electronic features for working in complementary or single-standing counterparts to approach more efficient results in comparison with the conventional materials and methods [5–8]. Accordingly, several efforts were done for investigating modifications and reconstructions of nanostructures after the pioneering carbon nanostructures for developing the targeted materials for the specific purposes [9–12]. Especially in the case of human related systems and therapies, several remarkable advantages were found for the nanostructures to be involved in various types of therapeutic applications [13–16]. Additionally, the correct recognition of external substances was supposed as one of the remarkable functions of nanostructures regarding their sensing and detecting activities [17–20]. Indeed, the wide surface area of nanostructures was seen very useful for providing an appropriate interaction media for adsorbing other substances and storages [21–24]. In this regard, several efforts were dedicated to learn details of such reactions and interactions, in which a general adsorbent phenomenon was developed for the functions of nanostructures [25–28]. Not only the pure carbon nanostructures, but also their modifications and derivatives yielded more efficient features for involving in the specific applications and functions towards a selective substance [29–32]. To this aim, the structural and electronic features were used to recognize the considered models to show their availability and related functions [33–36]. Accordingly, several architectures and compositions were suggested for the nanostructures and their features were analyzed to characterize them for a desired function [37–40]. Among such investigated systems and models, atomic doped nanostructures were found interesting by the useful impact of doped region for managing the electronic

* Corresponding author.
E-mail address: mdai.umsid@gmail.com (M. Da'i).

https://doi.org/10.1016/j.chphi.2023.100306
2667-0224/© 20XX

properties and activities of nanostructures in interactions with other substances [41–43]. In this regard, the doped region part could work as a moderator of interaction/adsorption process between the communicating counterparts [44–46]. The results of earlier works indicated benefits of employing the atomic doped nanostructures for adsorbing the external substances in a more suitable condition than the original pure nanostructures [47–49]. To do such analyses and recognitions, the computational tools were found among the most versatile techniques for providing informative insights into the investigated systems [50–54]. Accordingly, the current research work was done to investigate an issue of a formaldehyde chemical substance adsorption by the assistance of a doped model of fullerene nanostructure along with quantum computations.

Dealing with chemical pollutants has been always one of the main problematic issues for both of environments and human health systems [55–57]. Unfortunately, the existence of pollutants is not sometimes temporary and they will remain in the environment for years with different direct and indirect harmful impacts for the normal health systems [58–60]. In this regard, developing sensor materials of such harmful pollutants for their detection and removal is a crucial step for sustaining the biological systems [61–63]. To this aim, examining the sensitive adsorbent materials and customizing them for adsorbing the specific substances could help to approach a success for the detection and removal purposes [64–66]. Accordingly, the sensor function of a doped fullerene nanostructure was assessed in this work towards one of the most available chemical pollutants; formaldehyde, in the waste of all of chemical laboratories and industries [67]. Because of rapidly spreading in the environment, formaldehyde itself became a pollutant besides its very important role for participating in so many chemical reactions and productions [68]. To this point, a representative model of boron-nitrogen decorated carbon (BNC) fullerene nanostructure was investigated in the current work to assess the sensing process of formaldehyde (FMA) substance through the occurrence of possible interaction/adsorption processes. The fullerene and fullerene-like particles were found as single-standing nanostructures especially for involving in the interaction/adsorption processes [69–71]. The considered models were characterized by optimizing the geometries and evaluating the structural and electronic features to approach two important sensing terms of "recovery times" and "conductance rate" for the investigated adsorbing system [72]. The investigated models were analyzed based on the evaluated computational results as summarized in Tables 1-3 and Figs. 1-3.

Computational details

Models of this work including the representative pure C_{20} carbon fullerene (C) and its boron-nitrogen decorated derivative (BNC) were optimized to obtain their minimized energy geometries. Next, the interactions between each of already optimized C and BNC fullerenes and the formaldehyde (FMA) substance were re-optimized to obtain the minimized energy complexes; FMA@C and FMA@BNC (Fig. 1). Afterwards, details of interactions were extracted employing the quantum theory of atoms in molecules (QTAIM) approach to detect the types and features of involving interactions in the complexes [73]. Additionally, energetic features of the structures and also those of the frontier molecular orbitals were evaluated to learn the specifications of models regarding their structural and electronic terms. To this point, the complex

Table 1
Interaction/adsorption features of FMA@C and FMA@BNC complexes.

Complex	E_A kcal/mol	Int.	Dis. Å	Rho au	Del²-Rho au	H au
FMA@C	−2.21	O…C	2.85	0.0125	0.0344	0.0058
		H…C	2.71	0.0086	0.0237	0.0011
FMA@BNC	−22.39	O…B	1.56	0.1119	0.5128	−0.0601
		H…N	2.35	0.0483	0.2936	0.0081

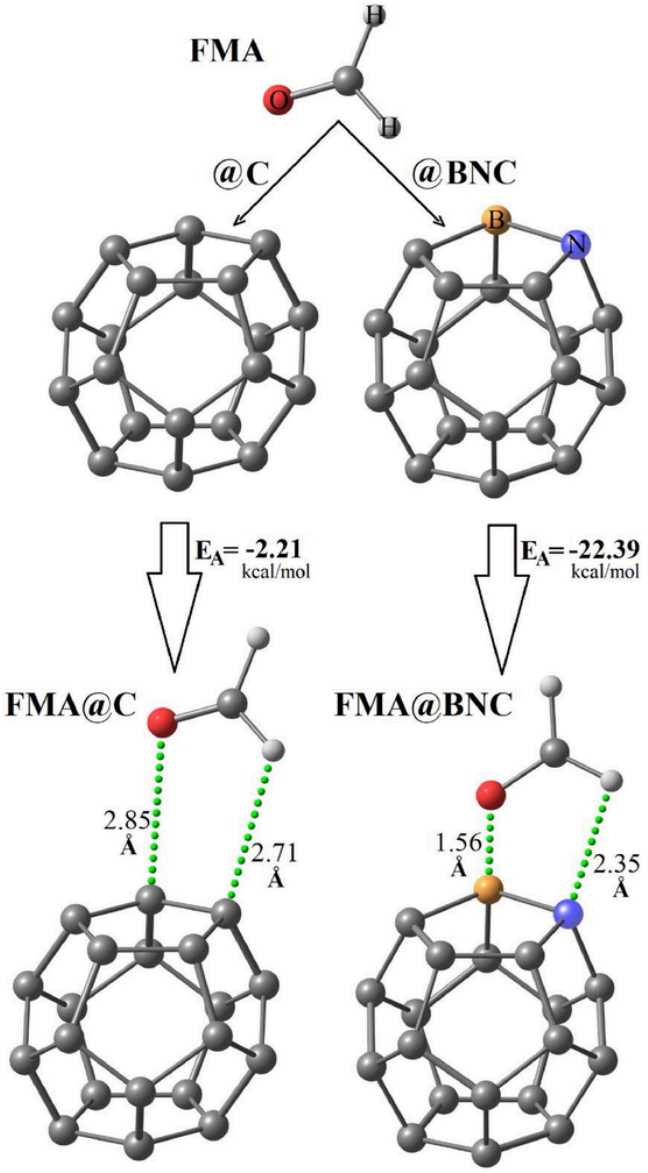

Fig. 1. Investigated models of this work including parental FMA, C, and BNC fullerenes and the interacting FMA@C and FMA@BNC complexes.

models were analyzed by the interaction/adsorption energy of counterparts (E_A) to yield the strength of complexes formations as indicated by Eq. (1). The impact of basis set super position error (BSSE) on the value of E_A was also implemented in the equation [74].

$$E_A = E_{Complex} - -E_{FMA} - -E_{Fullerene} + BSSE \quad (1)$$

Next, the energetic features of frontier molecular orbitals were extracted based on dominant energy levels of the highest occupied and the lowest unoccupied molecular orbitals (HOMO and LUMO) as indicated by Eqs. (2) - (5). The values of energy gap (GAP),%ΔGAP, chemical potential (C_p), and chemical hardness (C_H) were obtained accordingly. Additionally, distribution patterns of HOMO and LUMO and the visualized electrostatic potential (ESP) surfaces of models were exhibited in Fig. 2 besides showing the illustrated diagrams of density of states (DOS) in Fig. 3. The evaluated results of E_A and QTAIM features of complexes including the types of involving interactions and their specifications; density of all electrons (Rho), Laplacian of electron density (Del²-Rho), and energy density (H), were summarized in Table 1. The effects of existing solvents media on the stabilities of complexes (ΔG) were also recognized by calculating the Gibbs free energy features

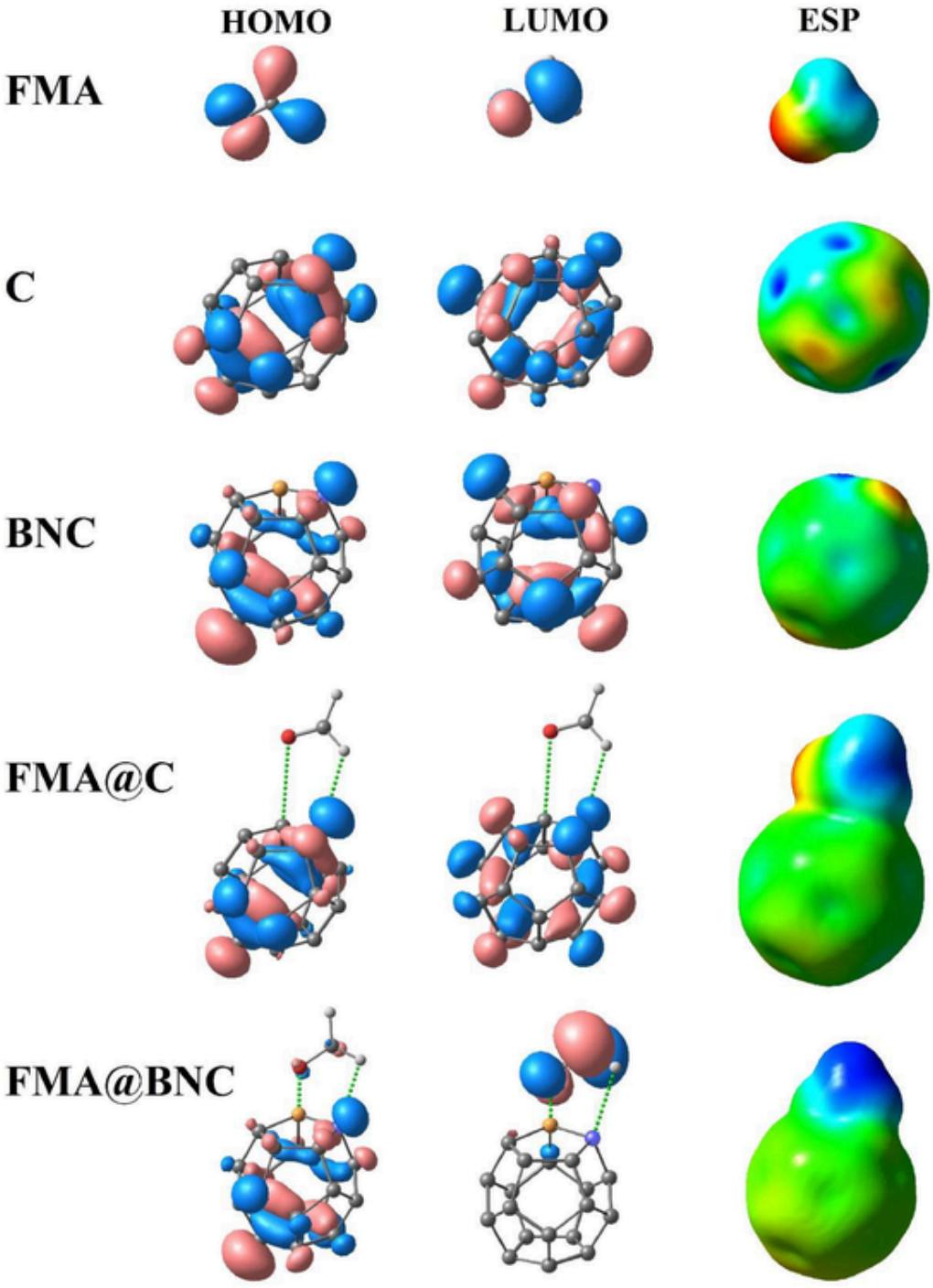

Fig. 2. Distribution patterns of HOMO and LUMO and ESP of FMA, C, BNC, FMA@C, and FMA@BNC models.

in gas, oil, and water media using the polarizable continuum model (PCM) and the results were listed in Table 2 [75]. Next, the frontier molecular orbital features were summarized in Table 3 to assess the structures based on their electronic specifications especially in the states of before and after complex formations. Indeed, two important terms of "recovery time" and "conductance rate" are mainly dependent on the values of E_A and GAP, respectively [72]. Accordingly, these features could be used to assess the sensing function of employed fullerenes for working towards the interaction/adsorption of FMA substance for revealing more insights into the developments of novel sensor materials for the chemical pollutants. To this point, the current computational work was explored by performing the wB97XD/6–31G* quantum chemical density functional theory (DFT) calculations using the Gaussian program in the 0 and 1 states of charge and multiplicity [76–78]. The evaluated vibrational frequencies of optimized models were also exhibited in the supplementary material. As a consequence, the required data were evaluated and they were discussed to reach a point of clearance for the investigated models systems by the advantages of employing computational research tools and methodologies for solving the scientific and even the industrial problems in a clear state [79–83].

$$\mathrm{GAP} = \mathrm{LUMO} - -\mathrm{HOMO} \tag{2}$$

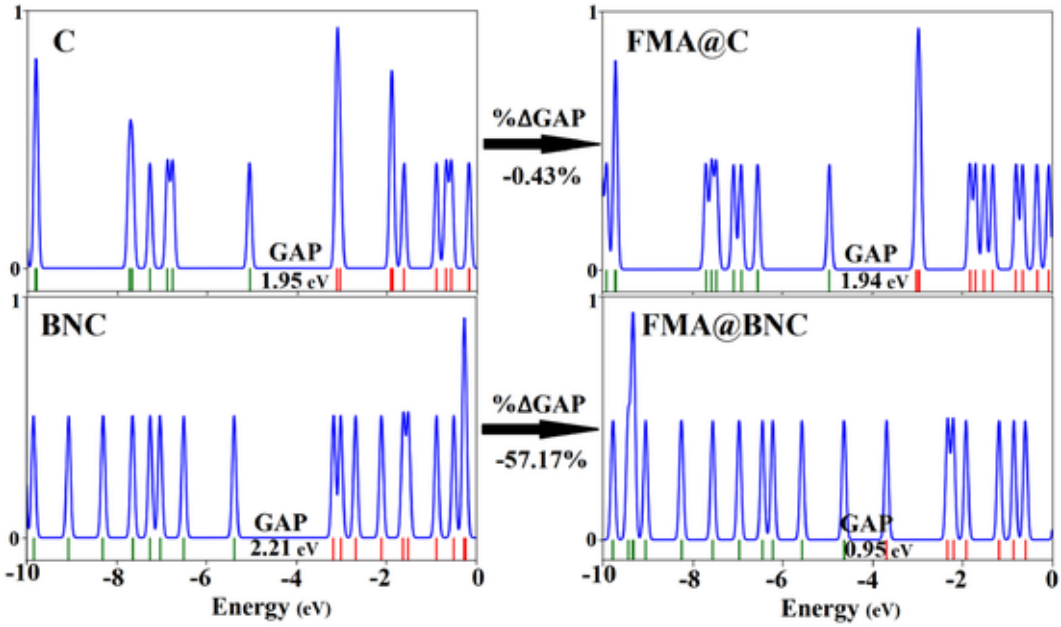

Fig. 3. Illustrated DOS diagrams of C, BNC, FMA@C, and FMA@BNC models.

Table 2
Differences of Gibbs free energy of FMA@C and FMA@BNC complexes in gas, oil, and water media.

Complex	$\Delta G_{Oil\text{-}Gas}$ kcal/mol	$\Delta G_{Water\text{-}Gas}$ kcal/mol	$\Delta G_{Oil\text{-}Water}$ kcal/mol
FMA@C	−1.61	−2.08	0.48
FMA@BNC	−7.01	−8.27	1.27

Table 3
Frontier molecular orbitals features of optimized models.

Model	HOMO eV	LUMO eV	GAP eV	%ΔGAP	C_P eV	C_H eV
FMA	−7.31	−1.15	6.16	n/a	−4.23	3.08
C	−5.05	−3.11	1.95	n/a	−4.08	0.97
BNC	−5.38	−3.16	2.21	n/a	−4.27	1.11
FMA@C	−4.95	−3.01	1.94	−0.43	−3.98	0.97
FMA@BNC	−4.63	−3.68	0.95	−57.17	−4.16	0.47

$$\%\Delta GAP = 100 \times \left[\left(GAP_{Complex} - \right.\right. \\ \left.\left. -GAP_{Fullerene}\right) / GAP_{Fullerene}\right] \quad (3)$$

$$C_P = (LUMO + HOMO)/2 \quad (4)$$

$$C_H = (LUMO - HOMO)/2 \quad (5)$$

Results and discussion

Considering the importance of developing novel sensor materials for detection and removal of chemical pollutants led to the performance of this work to explore a BN-decorated carbon (BNC) fullerene scaffold for sensing the formaldehyde (FMA) substance. Indeed, the potential features of nanostructures and their derivatives for involving in interaction/adsorption processes encouraged the researchers to explore their novel functions especially for working in the sensor materials. On the other hand, customizing a nanostructure for adsorbing a chemical species could be known as a crucial step of developing such needed materials. To this aim, learning details of interacting systems is very crucial to propose the nanostructures for the specific target applications. In this regard, all of covalent and non-covalent interactions should be known for determining the level of structural stability of complex formations between the pollutant adsorbate and the nanostructure adsorbent in addition to monitoring the electronic variations through the complex formations. Accordingly, performing molecular computations could yield details of structural and electronic features for the investigating systems to recognize variations before and after the occurrence of interaction/adsorption processes. Providing the informative descriptors for the molecular systems could reveal insights into the development of novel materials for the specific supplications, in which involving communications between FMA and BNC were investigated in this work based on the evaluated descriptors (Tables 1-3 and Figs. 1-3).

Within the current work, the evaluated computed features were used to analyze the models for revealing the sensor function specifications of the BNC adsorbent towards the FMA adsorbate. The structural models were shown in Fig. 1 as they were divided into parental single models of C and BNC fullerenes to interact with the FMA substance to create the bimolecular models of interacting FMA@C and FMA@BNC complexes. The involving interactions and their specifications for the optimized interacting configurations were analyzed based on the evaluated QTAIM features in addition to the interaction/adsorption energy (E_A) terms. Based on the quantitative results of Table 1 and the exhibited models of Fig. 1, the successful formations of both of FMA@C and FMA@BNC complexes were indicated along with the recognition of their specifications by the involving interactions and energy terms. A quick look at the geometries of complexes in Fig. 1 could reveal the distance of molecular counterparts from each other, in which the counterparts were optimized in a closer distance to each other in the FMA@BNC model in comparison with the FMA@C model. But it should be mentioned that the models were in suitable states regarding the energy values and the formations of both complexes were confirmed by the evaluated QTAIM features. Comparing the E_A of FMA@C (−2.21 kcal/mol) and FMA@BNC (−22.39 kcal/mol) complexes indicated the occurrence of a stronger interaction/adsorption process for the formation of FMA@BNC complex in comparison with the FMA@C complex. Accordingly, loser distances of counterparts were found in the FMA@BNC complex than those of the FMA@C complex. The B and N atomic decoration of pure carbon structure of C fullerene yielded an interactive surface for the BNC fullerene towards the FMA polar substance. Indeed, this BN-decoration enhanced the BNC fullerene for working as more appropriate surface for adsorbing the FMA substance in comparison with the pure C fullerene. However, the pure C fullerene was still able to adsorb the FMA substance to show the expected potential application of nanostructures for working as adsorbents, in which

the BN-decoration enhanced it for working as a more appropriate surface for approaching the desired purpose through the formation of a stronger FMA@BNC complex.

The features of QTAIM analyses indicated the existence of O…C (2.85 Å) and H…C (2.71 Å) interactions in the FMA@C complex from the FMA counterpart to the C counterpart. On the other hand, O…B (1.56 Å) and H…N (2.35 Å) interactions were found in the FMA@BNC complex from the FMA counterpart to the BNC counterpart. In this step, the models were detected by their involving interactions with a higher electron concentration for the interactions of FMA@BNC complex in comparison with the FMA@C complex based on the Rho and Del^2-Rho features of Table 1. Accordingly, observing a significant H value (−0.0601 au) indicated the O…B interaction as the strongest one among the complexes and the H…N interactions was placed at the next level of strength (H = 0.0081 au). For the case of FMA@C complex, O…C (H = 0.0058 au) and H…C (H = 0.0011 au) interactions were placed at the next levels of strength. This achievement could affirm a remarkable role of original C fullerene for the adsorption of FMA substance, in which the BN-decoration enhanced the fullerene for achieving a better result of interaction/adsorption process. As a consequence, the idea of BN-decoration for managing a successful adsorption of FMA substance was found achievable by comparing the obtained results of BNC and C fullerenes to see a stronger integration/adsorption process between the FMA and BNC counterparts.

After obtaining an approval of complex formations, the effects of oil and water solvents on the stability of complexes were also explored by evaluating the Gibbs free energy parameters in gas, oil, and water media. For running the calculations based on PCM approach, the isolated phase was implied for the gas phase, the 1-octanol dielectric constant included medium was implied for the oil phase, and the water dielectric constant included medium was implied for the water medium. Accordingly, the results were evaluated for comparing the stabilities of complex models in different phase media. The values of $\Delta G_{Oil\text{-}Gas}$, $\Delta G_{Water\text{-}Gas}$, and $\Delta G_{Oil\text{-}Water}$ were summarized in Table 2 as the variations of Gibbs values of each complex in the comparable media. For the FMA@C complex, the values of $\Delta G_{Oil\text{-}Gas}$, $\Delta G_{Water\text{-}Gas}$, and $\Delta G_{Oil\text{-}Water}$ were found as −1.61, −2.08, and 0.48 kcal/mol, respectively. This complex formation was defined by a better stability in both of oil and water media in comparison with the gas phase, in which the water medium was even more suitable for it in comparison with the oil medium. Because of formation of a bimolecular complex, a better interaction of molecular system with the involving medium was seen for both of oil and water medium with a priority of water medium. For the FMA@BNC complex, the values of $\Delta G_{Oil\text{-}Gas}$, $\Delta G_{Water\text{-}Gas}$, and $\Delta G_{Oil\text{-}Water}$ were found as −7.01, −8.27, and 1.27 kcal/mol, respectively, to show better features of BN-decorated model for stabilizing in the solvent media. The water medium was found better than the oil medium and the FMA@BNC model was able to be successfully achieved in both of oil and water solvents. As a consequence, both of FMA@C and FMA@BNC complexes could be still achievable in the solvent media with a higher priority of formation of the FMA@BNC complex in comparison with the FMA@C complex and a better suitability of the water solvent than the oil solvent as found by the values of Gibbs free energy for the complexes in different solvent media. It is worth to mention that the solvent effect will be implemented in the PCM-based calculations by the dielectric constants to be considered for the energy calculations resembling the existence of a molecule model in the solvent media [75].

Frontier molecular orbitals features of optimized models including the energy values of pure HOMO and LUMO levels and their related features such as GAP,%ΔGAP, C_P, and C_H were summarized in Table 3. In this step, the electronic variations of models before and after the interaction/adsorption processes were examined using the evaluated electronic features of models. For the original C and BNC fullerenes, the values of HOMO and LUMO were moved to lower levels as a result of BN-decoration enhancement in the BNC fullerene. However, the energy gap distance between HOMO and LUMO levels, as indicated by GAP, was farther in the BNC fullerene comparing to the C fullerene. The more conductive nature of pure C nanostructure was converted to the more semiconductor nature of BNC fullerene to be useful for employing in the sensor applications. The values of GAP in C (1.95 eV) and BNC (2.21 eV) fullerenes affirmed a more semiconductivity for the BNC fullerene comparing to the C fullerene. In this case, the values of C_P and C_H also showed such variations for the parental fullerene models due to the BN-decoration enhancement. The levels of HOMO and LUMO detected the new environment of complexes after the occurrence of interaction/adsorption processes, in which both levels detected the changes in both of FMA@C and FMA@BNC complexes. However, the amount of changes for the FMA@BNC fullerene was more significant than the FMA@C fullerene comparing to each other or comparing to the parental models. To assess such changes, the values of GAP indicated a very shorter distance between HOMO and LUMO levels in the FMA@BNC complex model whereas that of FMA@C complex was indeed very similar to the parental C fullerene model. The values of GAP for the parental C (1.95 eV) and BNC (2.212 eV) fullerenes were changed to new values in the FMA@C (1.94 eV) and FMA@BNC (0.95 eV) complexes. The values of%ΔGAP showed such variations by indicating −0.43 % and −57.17 % for the changes of GAP values form the parental state to the complex state in the C and BNC related models. As a consequence, the BN-decorated fullerene model was found very much suitable for approaching a sensor material of FMA substance in comparison with the C fullerene. Regarding the values of C_P and C_H, more significant variations were found for the FMA@BNC complex in contrast with the FMA@C complex. This achievement was an approval of the initial idea of this work for enhancing the C fullerene though the BN-decoration to prepare the BNC fullerene for a successful adsorption of the FMA substance. Not only a stronger interaction/adsorption of FMA was found for the BNC fullerene, but also the electronic features indicated a better suitability of sensing functions for the BNC fullerene by assessing the electronic variations between the parental and complex models.

The distribution patterns in Fig. 2 exhibited the variations of HOMO and LUMO levels, in which similar patterns were found for the parental and complex models of C fullerene in contrast with significant changes of patterns for the parental and complex models of BNC fullerene. The LUMO pattern was almost located at the FMA counterpart and the fullerene was vacant in the FMA@BNC complex; however, both of HOMO and LUMO patterns were located at the surface of C fullerene in the FMA@C complex. Examining the ESP surfaces for the parental fullerenes could show a significance of BN-decoration enhancement by providing a positive center (blue color) and a negative center (red color) for the BNC fullerene in contrast with the mixed regions for C fullerene.

The opposite color points of FMA and BNC fullerene were in a strong interaction to form the FMA@BNC complex in comparison with a weaker formation of the FMA@C complex. However, the continuous ESP surface for both of FMA@C and FMA@BNC complexes indicated the successful formation of both complexes through the occurrence of meaningful interaction/adsorption processes. Additionally, the localization of LUMO at the FMA counterpart of FMA@BNC complex made that part of complex in a blue color mode to show the positive site or an electron vacant place of the complex. Regarding the HOMO and LUMO distribution patterns, the formation of complexes and their electronic features were found for providing more insights into the idea assessment of BN-decoration enhancement of C fullerene for working in a successful sensing function of FMA substance. Additionally, the variations of molecular orbital levels before HOMO and after LUMO for the parental fullerenes and complex models were illustrated in the DOS diagrams of Fig. 3.

As discussed above, electronic variations of the FMA@BNC complex were more significant than those of the FMA@C complex, in which the

DOS diagrams indicated such changes in a clear mode. Especially for the energy gap distance between HOMO and LUMO levels, that of FMA@BNC complex was very significant in comparison with the parental BNC fullerene whereas that of FMA@C complex was almost negligible in comparison with the parental C complex. Accordingly, the BN-decorated fullerene was a useful example of enhancing the C fullerene for working in a more appropriate situation for adsorbing the FMA substance. Returning to the crucial terms of "recovery time" and "conductance rate", both terms could be very well discussed for the parental fullerenes and complexes in a comparable mode. By the assistance of E_A values, the recovery time could be recorded for both fullerenes with a more significance for the BNC fullerene in comparison with the C fullerene by the existence of a higher strength of interaction/adsorption of FMA substance for the FMA@BNC complex formation in comparison with the FAM@C complex. Hence, the recovery time of FMA@BNC complex was supposed to be longer than that of FMA@C complex, but both of them were achievable. By the assistance of%ΔGAP values, the conductance rate could be recorded for both fullerenes still with a more significance for the BNC fullerene in comparison with the C fullerene. The change of GAP of C and FMA@BNC models was almost negligible, but that of BNC and FMA@BNC models was very significant. In this case, a better conductance rate could be recorded for the formation of FMA@BNC complex in comparison with the formation of FMA@C complex. To summarize such achievements, it should be noted that the formation of complex models yielded possibility of achieving recovery time and their electronic variations yielded the chance of recording the conductance rate. As a consequence, both terms of recovery time and conductance rate were achievable for the BN-decorated model very better than the C model as a significant benefit of employed enhancement. Indeed, the existence of other atomic compositions in the original nanostructures could enhance their capability for working in more applications, which was observed by obtaining more useful features for the BNC complex of this work.

Conclusions

Details of interaction/adsorption processes of FMA pollutant by the assistance of an enhanced BNC fullerene was investigated by performing DFT calculations. The models were optimized and their electronic features were evaluated for providing the required data to discuss the targeted goal. The BN-decoration enhancement of C fullerene yielded a longer GAP distance between HOMO and LUMO levels in the BNC fullerene in comparison with the pure C fullerene, in which such GAP helped to push forward a better sensing process of the FMA@BNC complex formation in comparison with the FMA@C complex formation. Indeed, the formation of both of FMA@C and FMA@BNC complexes was achieved, but the interaction/adsorption strength of FMA@BNC complex was more significant than that of the FMA@C complex. In this case, the QTAIM results indicated the existence of two interactions in each complex with a majority of strength and electronic features for the formation of FMA@BNC complex. The results showed that the models were detectable by the terms of recovery time and conductance rate, in which the BN-decoration enhanced the features of BNC fullerene to approach better results in comparison with the pure C fullerene. Additionally, examining the effects of solvent media on the stability of complexes showed highlighted features for the FMA@BNC complex in both of oil and water solvents especially for the water solvent. As a consequence, the BN-decorated C fullerene worked as an appropriate adsorbent towards the interaction/adsorption processes of sensing the FMA pollutant.

CRediT authorship contribution statement

M. Da'i : Conceptualization, Writing – original draft, Supervision. **M. Mirzaei :** Investigation, Writing – review & editing. **F. Toiserkani :** Methodology, Visualization, Writing – review & editing. **S.M. Mohealdeen :** Data curation, Software. **Y. Yasin :** Data curation, Validation. **M.M.S. Bekhit :** Funding acquisition, Methodology, Visualization. **R. Akhavan-Sigari :** Conceptualization, Writing – review & editing.

Declaration of Competing Interest

The authors declare that they have no known competing financial interests or personal relationships that could have appeared to influence the work reported in this paper.

Data availability

Data will be made available on request.

Acknowledgements

The authors would like to extend their sincere appreciation to the Researchers Supporting Project Number (RSPD2023R986), King Saud University, Riyadh, Saudi Arabia.

Supplementary materials

Supplementary material associated with this article can be found, in the online version, at doi:10.1016/j.chphi.2023.100306.

References

[1] S. Malik, K. Muhammad, Y. Waheed, Nanotechnology: a revolution in modern industry, Molecules 28 (2023) 661.
[2] J. Gulomov, O. Accouche, Gold nanoparticles introduced ZnO/perovskite/silicon heterojunction solar cell, IEEE Access 10 (2022) 119558.
[3] N. El Hassan, K. Jabbour, A.H. Fakeeha, Y. Nasr, M.A. Naeem, S.B. Alreshaidan, Al-Fatesh AS. PRODUCTION of carbon nanomaterials and syngas from biogas reforming and decomposition on one-pot mesoporous nickel alumina catalysts, Alexandria Eng. J 63 (2023) 143.
[4] I. Patra, F.H. Mohammed, A.K.O. Aldulaimi, D.A. Khudhair, Y.F. Mustafa, A novel and efficient magnetically recoverable copper catalyst [MNPs-guanidine-bis (ethanol)-Cu] for Pd-free Sonogashira coupling reaction, Synth. Commun 52 (2022) 1856.
[5] M.K. Hassanzadeh-Aghdam, J. Jamali, A hierarchical micromechanics framework for properties of discontinuous carbon fiber composites containing graphene nanosheets, J. Brazil. Soc. Mech. Sci. Eng 44 (2022) 318.
[6] A. Raza, M. Azab, Z.A. Baki, C. El Hachem, M.H. El Ouni, N.B. Kahla, Experimental study on mechanical, toughness and microstructural characteristics of micro-carbon fibre-reinforced geopolymer having nano TiO2, Alexandria Eng. J 64 (2023) 451.
[7] H. Wei, H. Moria, K.S. Nisar, R. Ghandour, A. Issakhov, Y.L. Sun, A. Kaood, M.M. Youshanlouei, Effect of volume fraction and size of Al2O3 nanoparticles in thermal, frictional and economic performance of circumferential corrugated helical tube, Case Stud Thermal Eng 25 (2021) 100948.
[8] Y. Chen, L. Feng, S.S. Jamal, K. Sharma, I. Mahariq, F. Jarad, A. Arsalanloo, Compound usage of L shaped fin and nano-particles for the acceleration of the solidification process inside a vertical enclosure (A comparison with ordinary double rectangular fin), Case Stud. Thermal Eng 28 (2021) 101415.
[9] N.H. Abu-Hamdeh, T. AlQemlas, Z.J. Talabany, Y.A. Rothan, A.H. Milyani, AEAMA. Elamin, Implicit numerical method for discharging of energy storage curved container in appearance of nanomaterial evaluating performance, J. Energy Storage 60 (2023) 106570.
[10] A.R. Faraji, N.B. Khoramdareh, S. Ahmadi, A. Gil, A. Farahanipour, Z. Hekmatian, Synthesis of magnetic Mn/Fe oxides derived from drinking water sludges from a one-pot solvothermal process for the degradation of tetracycline and mixed dyes: synergistic effect and mechanism study, J. Environ. Chem. Eng. 11 (2023) 109668.
[11] M.Z. Dehaghani, A. Salmankhani, A.H. Mashhadzadeh, S. Habibzadeh, O. Abida, M.R. Saeb, Fracture mechanics of polycrystalline beryllium oxide nanosheets: a theoretical basis, Eng. Fract. Mech 244 (2021) 107552.
[12] S.E. Ahmed, W. Al-Kouz, A.M. Aly, Finite element method (FEM) analyses of the entropy and convective process within an inclined porous T-shaped domain using nano-encapsulated phase change materials (NEPCMs), ZAMM - J. Appl. Mathemat. Mech. 103 (2023) e202100329.

[13] A.K.O. Aldulaim, N.M. Hameed, T.A. Hamza, Abed AA. The antibacterial characteristics of fluorescent carbon nanoparticles modified silicone denture soft liner, J. Nanostruct 12 (2022) 774.
[14] S. Ghouli, M.R. Ayatollahi, B. Bahrami, J. Jamali, In-situ optical approach to predict mixed mode fracture in a polymeric biomaterial, Theor. Appl. Fract. Mech. 118 (2022) 103211.
[15] L. Palomino-Asencio, E.C. Anota, E. Garcia-Hernandez, Insights on α-glucose biosensors/carriers based on boron-nitride nanomaterials from an atomistic and electronic point of view, ChemPhysChem 23 (2022) e202200310.
[16] A. Gholami, E. Shakerzadeh, E.C. Anota, A theoretical perspective on the adsorption performance of pristine and Metal-encapsulated B36N36 fullerenes toward the hydroxyurea and nitrosourea anticancer drugs, Inorg. Chem. Commun 148 (2023) 110326.
[17] M.T. Baei, Y. Kanani, V.J. Rezaei, A. Soltani, Adsorption phenomena of gas molecules upon Ga-doped BN nanotubes: a DFT study, Appl. Surf. Sci 295 (2014) 18.
[18] A. Soltani, M.R. Taghartapeh, H. Mighani, A.A. Pahlevani, R. Mashkoor, A first-principles study of the SCN− chemisorption on the surface of AlN, AlP, and BP nanotubes, Appl. Surf. Sci 259 (2012) 637.
[19] X. Liu, W. Zheng, R. Kumar, M. Kumar, J. Zhang, Conducting polymer-based nanostructures for gas sensors, Coord. Chem. Rev 462 (2022) 214517.
[20] S. Al-Asadi, F. Al-Qaim, Application of response surface methodology on efficiency of fig leaf activated carbon for removal of methylene blue dye, Eurasian Chem. Comm. 5 (2023) 794.
[21] S. Ahmad, S. Gouadria, K. Jabbour, A. Naz, S. Manzoor, M. Abdullah, M.Z. Ansari, H.H. Hegazy, S. Aman, M.N. Ashiq, Iron doped Gd2Zr2O7 hierarchical nanoflakes arrays as robust electrodes materials for energy storage application, J. Energy Storage 60 (2023) 106687.
[22] Y. Yang, K. Logesh, S. Mehrez, I. Huynen, I. Elbadawy, V. Mohanavel, S. Alamri, Rational construction of wideband electromagnetic wave absorber using hybrid FeWO4-based nanocomposite structures and tested by the free-space method, Ceram. Int 49 (2023) 2130.
[23] M.K. Hassanzadeh-Aghdam, R. Ansari, J. Jamali, H. Mohaddes Deylami, Heat transfer characteristics in discontinuous silicon carbide-reinforced aluminum multiphase composites containing nano-graphene additives: a micromechanics-based multistep technique, J. Brazilian Soc. Mech Sci. Eng 44 (2022) 344.
[24] N.H. Abu-Hamdeh, S.M. Alghamdi, Z.J. Talabany, Y.A. Rothan, T. AlQemlas, A. Musa, Numerical thermal storage analysis within discharging involving nanomaterial, J. Energy Storage 59 (2023) 106530.
[25] E. Salehi, M. Khajavian, N. Sahebjamee, M. Mahmoudi, E. Drioli, T. Matsuura, Advances in nanocomposite and nanostructured chitosan membrane adsorbents for environmental remediation: a review, Desalination 527 (2022) 115565.
[26] S. Pour Karim, R. Ahmadi, M. Yousefi, K. Kalateh, G Zarei, Interaction of graphene with amoxicillin antibiotic by in silico study, Chem. Methodolog. 6 (2022) 861.
[27] S. Noor, A. Al-Shamari, High photocatalytic performance of ZnO and ZnO/CdS nanostructures against reactive blue 4 dye, Eurasian Chem. Comm. 5 (2023) 776.
[28] E. Golipour-Chobar, F. Salimi, G. Ebrahimzadeh-Rajaei, Sensing of lomustine drug by pure and doped C48 nanoclusters: DFT calculations, Chem. Methodolog 6 (2022) 790.
[29] M.S. Villanueva, A.B. Hernandez, E. Shakerzadeh, E.C. Anota, Effect of global charge on stability and electronic properties of B36N36 cage and isomers, Physica. E 152 (2023) 115758.
[30] M.Z. Dehaghani, F. Molaei, F. Yousefi, S.M. Sajadi, A. Esmaeili, A. Mohaddespour, O. Farzadian, S. Habibzadeh, A.H. Mashhadzadeh, C. Spitas, M.R. Saeb, An insight into thermal properties of BC3-graphene hetero-nanosheets: a molecular dynamics study, Sci. Rep 11 (2021) 23064.
[31] P. Sharma, J. Prakash, R. Kaushal, An insight into the green synthesis of SiO2 nanostructures as a novel adsorbent for removal of toxic water pollutants, Environ. Res. 212 (2022) 113328.
[32] R.M. Shahzad, H.F. Fard, I. Mahariq, M.E. Assad, Al-Shabi MA, Thermal conductivity prediction of nanofluids containing SiC particles by using artificial neural network, Energy Harvest. Storage: Mater. , Dev. Appl. XII 12090 (2022) 31.
[33] L. Kolsi, A.K. Hussein, W. Hassen, L. Ben Said, B. Ayadi, W. Rajhi, T. Labidi, A. Shawabkeh, K Ramesh, Numerical study of a phase change material energy storage tank working with carbon nanotube–water nanofluid under Ha'il city climatic conditions, Mathematics 11 (2023) 1057.
[34] A. Venkateswarlu, N. Murshid, H. Mulki, M. Abu-samha, S. Suneetha, M.J. Babu, C.S. Raju, R.Z. Homod, Al-Kouz W. A significant role of activation energy and fourier flux on the quadratically radiated sphere in low and high conductivity of hybrid nanoparticles, Symmetry 14 (2022) 2335.
[35] B. Mourched, N. Ferko, M. Abdallah, B. Neji, S. Vrtagic, Study and design of a machine learning-enabled laser-based sensor for pure and sea water determination using COMSOL multiphysics, Applied Sci. 12 (2022) 6693.
[36] M. Shams, N. Kausar, S. Kousar, D. Pamucar, E. Ozbilge, B. Tantay, Computationally semi-numerical technique for solving system of intuitionistic fuzzy differential equations with engineering applications, Adv. Mech. Eng 14 (2022) 16878132221142128.
[37] F. Ali, S. Fazal, N. Iqbal, A. Zia, F Ahmad, PANI-based nanocomposites for the removal of dye from wastewater, Asian J. NanoSci. Mater. 6 (2023) 106.
[38] E. Mahal, S. Al-Mutlaq, Bio-based carbon nanomaterials synthesis from waste tea, Eurasian Chem. Comm. 5 (2023) 264.
[39] M.B. Al Taee, B.M Al Shabander, Study the effect of ZnO concentrations on the photocatalytic activity of TiO2/cement nanocomposites, Chem. Methodolog. 6 (2022) 831.
[40] A. Belhachem, N. Amara, H. Belmekki, Y. Yahia, Z. Cherifi, A. Amiar, A. Bengueddach, R. Meghabar, H. Toumi, Synthesis, characterization and anti-inflammatory activity of an alginate–zinc oxide nanocomposite, Asian J. NanoSci. Mater. 6 (2023) 173.
[41] N. Farhami, A computational study of thiophene adsorption on boron nitride nanotube, J. Applied Organomet. Chem. 2 (2022) 148.
[42] S.S. Moayeripour, R. Behzadi, Experimental investigation of the effect of titanium nano-particles on the properties of hydrophobic self-cleaning film, Eurasian Chem. Comm 5 (2023) 303.
[43] K. Harismah, M. Mirzaei, Complex formations of favipiravir and BeO-decorated carbon nanocones along with quantum processing, Biointerface Res. Applied Chem. 13 (2023) 508.
[44] M. Da'i, Wahyuni AS Maryati, E.R. Wikantyasning, M Mirzaei, Vitamin-B3 adsorption by a Ti-doped graphene, Biointerface Res. Applied Chem. 13 (2023) 482.
[45] M.J. Ansari, G. Widjaja, W. Suksatan, Altimari US, Abd ALhusain AK. Investigating fullerene-oxide nanostructure as an adsorbent of ammonia: complexation efficiency by density functional theory, Main Group Chem. 21 (2022) 671.
[46] M. Ahmadlouydarab, S. Javadi, A.A.F. Darab, Evaluation of thermal stability of TiO2 applied on the surface of a ceramic tile to eliminate methylene blue using silica-based doping materials, Adv. J. Chem. Section A 6 (2023) 352.
[47] M.J. Saadh, S.S. Abdullaev, J.M. Falcon-Roque, R.D. Cosme-Pecho, R.Y. Castillo-Acobo, M. Obaid, M. Mohany, S.S. Al-Rejaie, M. Mirzaei, M. Da'i, K. Harismah, Sensing functions of oxidized forms of carbon, silicon, and silicon-carbon nanocages towards the amantadine drug: DFT assessments, Diam. Relat. Mater 137 (2023) 110137.
[48] Rad F Arjomandi, J. Talat Mehrabad, M. Dizaji Esrafili, A communal experimental and DFT study on structural and photocatalytic properties of nitrogen-doped TiO2, Adv. J. Chem. Sec. A 6 (2023) 244.
[49] J. Islam, A. Kumer, U. Chakma, M.M. Alam, S. Biswas, Z. Ahmad, M.S. Islam, M.I.J. Jony, M.B. Ahmed, Investigation of structural, electronic, and optical properties of SrTiO3 and SrTi0.94Ag0.06O3 quantum dots based semiconductor using first principle approach, Adv. J. Chem. Sec. A 5 (2022) 164.
[50] R. Ghiasi, F. Aghazadeh Kozeh Kanani, Theoretical insights of the electronic structures, conductivity, and aromaticiy of graphyne and Si-doped graphynes, Asian J. NanoSci. Mater. 5 (2022) 303.
[51] S. Ariavand, M. Ebrahimi, E. Foladi, Design and construction of a novel and an efficient potentiometric sensor for determination of sodium ion in urban water samples, Chem. Methodolog. 6 (2022) 886.
[52] M.N. Sidik, Y. Mhd Bakri, S.S. Syed Abdul Azziz, A.K.O. Aldulaimi, C.F. Wong, M Ibrahim, In silico xanthine oxidase inhibitory activities of alkaloids isolated from alphonsea sp, S. Afr. J. Bot. 147 (2022) 820.
[53] S. Esfahani, J. Akbari, S. Soleimani-Amiri, M. Mirzaei, A.G. Gol, Assessing the drug delivery of ibuprofen by the assistance of metal-doped graphenes: insights from density functional theory, Diam. Relat. Mater 135 (2023) 109893.
[54] Rezaei Sameti M, B Amirian, A quantum, NBO, RDG study the interaction of cadmium ion with the pristine, C, P and C&P doped (4,4) armchair boron nitride nanotube (BNNTs), Asian J. NanoSci. Mater. 5 (2022) 327.
[55] T. Münzel, O. Hahad, A. Daiber, P.J. Landrigan, Soil and water pollution and human health: what should cardiologists worry about? Cardiovasc. Res. 119 (2023) 440.
[56] E. Novita, A.Z. Karomi, H.A. Pradana, Spatial distribution of potential pollution load point source of bedadung river in the urban area segment, Forum Geografi 36 (2022) 110.
[57] E. Saptutyningsih, A Ma'ruf, Measuring the impact of urban air pollution: hedonic price analysis and health production function, Jurnal Ekonomi Pembangunan: Kajian Masalah Ekonomi Dan Pembangunan 16 (2015) 146.
[58] H.T. Mohammed, K.K. Alasedi, R. Ruyid, S.A. Hussein, A.L. Jarallah, S.M.A. Dahesh, M.Q. Sultan, Z.N. Salman, B.S. Bashar, A.K.O. Aldulaimi, M.A. Obaid, ZnO/Co3O4 nanocomposites: novel preparation, characterization, and their performance toward removal of antibiotics from wastewater, J. Nanostruct. 12 (2022) 503.
[59] H.A. Kareem, M. Zaidi, A.A. Baqer, S.K. Hachim, T. ghazuan, K.K. Alasedi, et al., Synthesis and characterization of CoFe2O4 nanoparticles and its application in removal of reactive violet 5 from water, J. Nanostruct 12 (2022) 521.
[60] R. Bibi, Z. Muhammad, Z. Ahmad, F. Ahmad, A comprehensive screening of toxic heavy metals in the water of FATA (Pakistan), J. Chem. Rev 5 (2023) 281.
[61] N. Agasti, V. Gautam, N. Pandey, M. Genwa, P.L. Meena, S. Tandon, R. Samantaray, Carbon nanotube based magnetic composites for decontamination of organic chemical pollutants in water: a review, Applied Surface Sci. Advances 10 (2022) 100270.
[62] Y. Zhang, Y. Zhu, Z. Zeng, G. Zeng, R. Xiao, Y. Wang, Y. Hu, L. Tang, C Feng, Sensors for the environmental pollutant detection: are we already there? Coord. Chem. Rev 431 (2021) 213681.
[63] G. Chala, Review on green synthesis of iron-based nanoparticles for environmental applications, J. Chem. Rev 5 (2023) 1.
[64] M. Mirzaei, E. Karimi, M. Yousefi, BN nanoflake for hazardous SO2 gas capturing: DFT study, Biointerface Res. in Applied Chem. 12 (2022) 359.
[65] B. Ghanavati, A. Bozorgian, Removal of copper II from industrial effluent with beta zeolite nanocrystals, Prog. Chem. and Biochem.Res. 5 (2022) 53.
[66] O. Ajayi, M. Bowaje, A. Ojo, B. Ogunnaiya, E. Idowu, S. Oni, O. Ajayi, B. Dosunmu, A review on natural clay application for removal of pharmaceutical residue in wastewater, Prog. Chem. and Biochem.Res. 6 (2023) 71.
[67] T. Salthammer, Formaldehyde in the ambient atmosphere: from an indoor pollutant to an outdoor pollutant? Angew. Chem. Int. Ed. 52 (2013) 3320.
[68] M.B. Henda, S.H. Sadon, Z. Li, Q.H. Le, Removal of formaldehyde pollutant from

petroleum industry wastewaters by polymers: a molecular dynamics simulation, Eng. Anal. Bound. Elem 151 (2023) 400.
[69] A.V. Baskar, M.R. Benzigar, S.N. Talapaneni, G. Singh, A.S. Karakoti, J. Yi, A.A. Al-Muhtaseb, K. Ariga, P.M. Ajayan, A. Vinu, Self-assembled fullerene nanostructures: synthesis and applications, Adv. Funct. Mater. 32 (2022) 2106924.
[70] S. Yeasmin, M. Mehade Hasan, A.A. Oishi, S.A. Bithe, D. Roy, A.S Rad, A first principles study of adsorption of hydrazine on C20, C40 and C60 fullerene nanoclusters, Mol. Simul 49 (2023) 551.
[71] M. Da'i, E.R. Wikantyasning, Wahyuni AS Maryati, M Mirzaei, A titanium-enhanced boron nitride fullerene for the drug delivery of 5-fluorouracil anticancer: DFT study, Biointerface Res. Applied Chem. 13 (2023) 434.
[72] M. Heidari, M. Solimannejad, The porous B6N6 boron nitride covalent organic framework as a potential platform for sensing and delivering lomustine anticancer drug: a first-principles study, J. Inorg. Organomet. Polym. Mater 32 (2022) 4216.
[73] R.F. Bader, T.T. Nguyen-Dang, Quantum theory of atoms in molecules–Dalton revisited, Adv. Quantum Chem. 14 (1981) 63.
[74] E.R. Davidson, S.J. Chakravorty, A possible definition of basis set superposition error, Chem. Phys. Lett 217 (1994) 48.
[75] B. Mennucci, Polarizable continuum model, Wiley Interdisciplinary Rev.: Computat. Mol. Sci. 2 (2012) 386.
[76] M.M. Francl, W.J. Pietro, W.J. Hehre, J.S. Binkley, M.S. Gordon, D.J. DeFrees, J.A. Pople, Self-consistent molecular orbital methods. XXIII. A polarization-type basis set for second-row elements, J. Chem. Phys 77 (1982) 3654.
[77] V.A. Rassolov, M.A. Ratner, J.A. Pople, P.C. Redfern, L.A. Curtiss, 6-31G* basis set for third-row atoms, J. Comput. Chem 22 (2001) 976.
[78] M.J. Frisch, G.W. Trucks, H.B. Schlegel, G.E. Scuseria, M.A. Robb, J.R. Cheeseman, et al., Gaussian 09 Program, Gaussian Inc., Wallingford, CT, 2009.
[79] G.R. Schleder, A.C. Padilha, C.M. Acosta, M. Costa, A. Fazzio, From DFT to machine learning: recent approaches to materials science–a review, J. Physics: Mater. 2 (2019) 032001.
[80] A. Al-Sarray, Molecular and electronic properties of Schiff bases derived from different aniline derivatives: density functional theory study, Eurasian Chem. Comm. 5 (2023) 317.
[81] S.A. Aghaward, L.J. Abbas, K.A. Hussein, Synthesis, characterisation, and biological and computational studies of novel schiff bases from heterocyclic molecules, J. Medicinal and Chem. Sci. 6 (2023) 1714.
[82] A. Heidaripour, F. Salmani, Study of PbS quantum dots (QDs) and proposing Pb@PbS-QD@CdSe for new generation of LEDs, Asian J. Green Chem. 7 (2023) 15.
[83] S. Kirkok, J. Kibet, T. Kinyanjui, F Okanga, A mechanistic formation of phenolic and furan-based molecular products from pyrolysis of model biomass components, Prog. Chem. Biochem.Res. 5 (2022) 376.